Received: 27 June 2022 | Revised: 13 September 2022 | Accepted: 27 September 2022

DOI: 10.1002/aoc.6926

FULL PAPER

Applied Organometallic Chemistry WILEY

Green synthesis of Zn nanoparticles and in situ hybridized with BSA nanoparticles for Baicalein targeted delivery mediated with glutamate receptors to U87-MG cancer cell lines

Mahmoud Gharbavi[1] | **Behrooz Johari**[2,3] | **Roghayeh Ghorbani**[2] | **Hamid Madanchi**[4] | **Ali Sharafi**[3,5]

[1]Nanotechnology Research Center, Ahvaz Jundishapur University of Medical Sciences, Ahvaz, Iran

[2]Department of Medical Biotechnology, School of Medicine, Zanjan University of Medical Sciences, Zanjan, Iran

[3]Zanjan Pharmaceutical Biotechnology Research Center, Zanjan University of Medical Sciences, Zanjan, Iran

[4]Department of Biotechnology, School of Medicine, Semnan University of Medical Sciences, Semnan, Iran

[5]School of Pharmacy, Zanjan University of Medical Sciences, Zanjan, Iran

Correspondence
Behrooz Johari, Department of Medical Biotechnology, School of Medicine, Zanjan University of Medical Sciences, Zanjan, Iran.
Email: dr.johari@zums.ac.ir and behroozjohari@yahoo.com

Ali Sharafi, Zanjan Pharmaceutical Biotechnology Research Center, Zanjan University of Medical Sciences, Zanjan, Iran.
Email: alisharafi@zums.ac.ir and sharafi.a@gmail.com

Glioblastoma multiforme (GBM) is the most aggressive malignant tumor of the brain. It has different glutamate receptor types. So, these receptors can be a suitable target for GBM treatment. The current study investigated the anticancer effects of bovine serum albumin (BSA)-Baicalein @Zn-Glu nanostructure mediated-GluRs in human glioblastoma U87 cells. BSA-Ba@Zn-Glu hybrid nanoparticles (NPs) were set and considered transporters for Baicalein (Ba) active compound delivery. BSA-Ba@Zn-Glu NPs were synthesized by a single-step reduction process. The successful production was confirmed through transmission electron microscopy (TEM), dynamic light scattering (DLS), Fourier transform infrared spectroscopy (FT-IR), and hemolysis test. The cytotoxic efficacy and apoptosis rate of the nanostructures on U87 glioblastoma cells were investigated by 3-(4,5-dimethylthialzol-a-yl)-2,5 diphenyltetrazolium bromide (MTT) and flow cytometry assays, respectively. The synthesized BSA-Ba@Zn-Glu nanostructures with a diameter of 142.40 ± 1.91 to 177.10 ± 1.87 nm and *zeta* potential of −10.57 ± 0.71 to −35.77 ± 0.60 mV are suitable for extravasation into tumor cells. The drug release from the BSA-Ba@Zn NPs showed controlled and pH-dependent behavior. In vitro results indicated that the BSA-Ba@Zn-Glu NPs significantly reduce cell viability and promote apoptosis of U87 cancer cells. It revealed the cytotoxic effect of the Baicalein and an increase in cellular uptake of nanoparticles by Glu receptors. Zn NPs were synthesized based on a green synthesis method. BSA NPs were used as a nano-platform for Glu conjugation and Ba drug delivery. BSA-Ba@Zn-Glu NPs induce cytotoxicity and apoptosis in human brain cancer cells

Abbreviations: AIC, Akaike's information of variance; Ba, Baicalein; BSA, bovine serum albumin; BSA-Ba NPs, Baicalein-loaded BSA NPs; BSA-Ba@Zn NPs, Zn NPs hybridized with BSA-Ba NPs; BSA-Ba@Zn-Glu NPs, Glu-conjugated BSA-Ba@Zn NPs; DLS, dynamic light scattering; DMEM, Dulbecco's Modified Eagle's Medium-high Glucose; DMSO, dimethyl sulfoxide; FBS, fetal bovine serum; FESEM, field emission scanning electron microscopy; FT-IR, Fourier-transform infrared spectroscopy; GBM, glioblastoma multiforme; GluRs, glutamate receptors; KARs, kainate receptors; KBr, potassium bromide; LE%, loading efficiency percentage; MSE, mean squared error; MTT, 3-(4,5-dimethylthialzol-a-yl)-2,5 diphenyltetrazolium bromide; NMDA, , N-methyl-D-aspartate; AMPA, AMP-activated protein kinase; PBS, phosphate-buffered saline; PDI, polydispersity index; RBCs, red blood cells; Z-average, average hydrodynamic diameter.

 © 2022 John Wiley & Sons, Ltd.

Funding information
The present study was supported by Zanjan University of Medical Sciences, Zanjan, Iran (grant number: A-12-1244-13 & ethical code: IR.ZUMS.REC.1399.326).

(U87) in a dose-dependent manner. Finally, this nanostructure could be served in targeted drug delivery in vivo studies and applied along with other strategies such as X-ray irradiation as combinational therapies in future studies.

KEYWORDS
Baicalein, drug delivery, glutamate receptors, green synthesis, Zn nanoparticles

1 | INTRODUCTION

Glioblastoma multiforme (GBM) is the most common primary malignant brain tumor and the most aggressive malignancy. The majority of patients die within 15–18 months, and less than 5% of them are alive at 5 years from diagnosis.[1–3] Glioblastoma can migrate into the healthy brain tissue, resulting in cancer spreading.[4] Furthermore, these tumors are also resistant to conventional treatments such as chemotherapy and radiation therapy.[5]

Nanotechnology is considered a new promising tool for cancer diagnosis, treatment, and targeting of cancer cells.[6] Drug delivery across the blood–brain barrier (BBB) toward brain tumors is a key concerning issue owing to the low permeability of active compounds. BBB mostly limits the entrance of all large molecules and more than 98% of small molecules into the brain tissue.[7] Nanoparticles (NPs) have attracted much interest because of the potential to avoid problems related to viral vector vehicles. Their physicochemical adaptability lets for tailoring of the NP surface for tumor targeting.[8] Bovine serum albumin (BSA) NPs are unique nanostructures for drug delivery because they are readily available, non-toxic, non-immunogenic, biocompatible, and biodegradable. They have many physical and biological advantages, including the inherent tendency to cancerous and inflamed tissues, being flexible in the body, better solubility, and bioavailability of therapeutic agents, in particular, lipophilic drugs, as well as they can protect the drug against destruction and inactivation by immunological and pharmacological effects.[9]

Green synthesis of metallic NPs has several advantages over conventional methods such as safety, cost-effectiveness, eco-friendliness, and biocompatibility.[10,11] In the current study, the Zn NPs were fabricated via green synthesis approach. This is one of the most attractive nanoparticles in medicine that have unique electrical, optical, catalytic, and photochemical properties with antimicrobial and antioxidant activity, which may lead to apoptosis and inhibition of cancer cell growth.[12]

It is known that glioma cells express inotropic glutamate receptors (GluRs), such as AMPA, N-methyl-D-aspartate (NMDA), and kainate receptors (KARs).[13,14] Hence, GluRs could be an effective target for efficient drug delivery for cancer treatment or imaging. Furthermore, natural antioxidants and many phytochemicals, due to their antiproliferative and pro-apoptotic properties, have been introduced as anticancer adjuvant drugs.[15,16] Baicalein (Ba) is one of the most essential flavonoids with several properties, including antiviral, antihepatic, anti-inflammatory, and antitumor effects.[17–19] It also shows antioxidant and inhibitory effects against glioblastoma multiform.[20] The suggested mechanism for induction of apoptosis by Ba is the increase of ROS and calcium ions, which alter the expression of Bax and Bcl2 genes and their ratios, leading to an increase in cytochrome c and activation of caspase-3, which leads to inducing apoptosis in cancer cells.[21]

In the present study, BSA NPs were used as a nanoplatform for Glu conjugation, Ba delivery, and simultaneously, they were utilized as a reducing factor for the green synthesis of Zn NPs, which hybridized with BSA NPs to form BSA-Ba@Zn-Glu as a suggested final nanosystem in this study. The synthesized hybrid nanostructures that targeted Glu were used to deliver Baicalein to U87-MG cancer cells. Finally, their effect on cell viability and apoptosis was evaluated.

2 | MATERIALS AND METHODS

2.1 | Reagents and materials

Zinc sulfate, glutamate (56-86-0), Baicalein, BSA, 1-ethyl-3-[3-(dimethylamino) propyl] carbodiimide (EDC; 25952-53-8), *N*-hydroxysuccinimide, Dulbecco's Modified Eagle's Medium-high Glucose (DMEM), fetal bovine serum (FBS), 3-(4,5-dimethylthialzol-a-yl)-2,5 diphenyltetrazolium bromide (MTT), penicillin–streptomycin, and trypsin–EDTA were obtained from Sigma-Aldrich Co. (St. Louis, MO, USA). Phosphate-buffered saline (PBS) was prepared in the laboratory. Dimethyl sulfoxide (DMSO), methanol, and acetone were obtained from Emertat chimi (Emertat Co., Iran). Annexin V PI kit was obtained from (Sigma). U87 MG cell line (ATCC HTB-14) was obtained from Bon Yakhteh Research Institute (Tehran, Iran).

2.2 | Green synthesis of Zn NPs

Zn NPs were produced by the redox reaction of zinc sulfate ($ZnSO_4 \cdot H_2O$) with BSA as a reducing factor, as previously described by Gharbavi et al. with some modifications.[22] Briefly, 4% w/v BSA, as a reducing agent, was dissolved in 5 ml PBS (pH 7.4) with 0.2% w/v of zinc sulfate, which was maintained at ambient temperature for 10 min under vigorous stirring to achieve a homogenous solution. Then, the NaOH (1 N) was immediately added to adjust the pH of the solution to 9 and maintained at 90°C under strong stirring. After 1 h, the color of the colloidal solution changed from a colorless to transparent yellow color. The colloidal solution was centrifuged at 700 rpm for 5 min to remove debris from BSA. Finally, the obtained colloidal solution was purified by dialysis using a 12-kDa molecular weight cutoff against ultrapure water for overnight to remove the excess zinc sulfate and other precursors.

2.3 | Synthesis of BSA NPs, Baicalein-loaded BSA NPs (BSA-Ba NPs), and Zn NPs hybridized with BSA-Ba NPs (BSA-Ba@Zn NPs)

BSA NPs and BSA-Ba NPs were synthesized by the modified desolation method.[23] Briefly, 100 mg BSA was added to 3.5 ml PBS (or 3.5 ml PBS with 0.01% Zn NPs to prepare BSA-Ba@Zn NPs) and kept at 40–50°C under vigorous stirring for 15 min. Next, 7 ml Ba solution with a concentration of 4 mg ml^{-1} (Ba/acetone solution) was dropwise added to each of the above solutions under constant stirring and dark conditions. After 40 min, 0.05% w/v EDC was added to the above solution to stabilize and cross-link the BSA NPs and kept overnight. Finally, the BSA-Ba NPs and BSA-Ba@Zn NPs were purified by repeated centrifugation and washed with PBS three times. BSA NPs were prepared by the same protocol with acetone instead of Ba/acetone solution.

2.4 | Synthesis of Glu-conjugated BSA-Ba@Zn NPs (BSA-Ba@Zn-Glu NPs)

EDC and NHS, as coupling reagents, were used in order to covalently bind Glu at the surface of BSA-Ba@Zn NPs. 1% w/v BSA-Ba@Zn NPs was dispersed in 10 ml PBS and mixed with 0.25% w/v Glu, 0.5% w/v EDC, and 0.3% w/v NHS. The pH of the resulting suspension was adjusted to 8.5 by the addition of the bicarbonate buffer and continuously stirred at ambient temperature. After 16 h, the final formulation (BSA-Ba@Zn-Glu NPs) was ready, and excess components were removed by extensive dialysis membranes (MWCO 12000).[24]

2.5 | Physicochemical characterizations of nanostructures

Physicochemical properties of nanostructures were characterized by dynamic light scattering (DLS), field emission scanning electron microscopy (FESEM), and Fourier-transform infrared spectroscopy (FT-IR) techniques. The average hydrodynamic diameter (Z-average), polydispersity index (PDI), and charge surface (*zeta* potential) of Zn NPs, BSA NPs, BSA@Zn NPs, BSA@Zn-Glu NPs, BSA-Ba NPs, BSA-Ba@Zn NPs, and BSA-Ba@Zn-Glu NPs were determined by DLS (Malvern NanoZS model). Two hundred microliters from each sample was diluted into 2 ml of deionized water until the absorbance at 633 nm reached 0.07 ± 0.02 units.

FESEM (MIRA TESCAN, Czech Republic) image was utilized to estimate the size and morphology of BSA-Ba@Zn-Glu NPs. The samples were covered with platinum and observed at 15 kV on a scale of 100,000× magnification.

The chemical structure and composition of all formulations, as well as free Baicalein and free Glu, were characterized by FT-IR (Bruker, Tensor 27). All samples were mixed and mechanical ground with potassium bromide (KBr) at a weight ratio of 1:10 to get pellets at 10 Ton pressure.

2.6 | Loading efficiency

The loading efficiency percentage (LE%) of Ba in prepared formulations (BSA-Ba NPs, BSA-Ba@Zn NPs, and BSA-Ba@Zn-Glu NPs) was calculated using the centrifugation method.[25] Briefly, all formulations were centrifuged at 14,000 rpm for 10 min to determine the amount of free Ba in the supernatant. The unloaded Ba was quantified using a UV–Vis spectrophotometer (Thermo Fisher Scientific) at a wavelength of 330 nm. Finally, Ba LE% was determined according to the following equation:

$$DL\% = \frac{W_{drug}}{W_{nanocarrier}} \times 100$$

where $DL\%$ is the drug-loading ratio (%) and W_{drug} and $W_{nanocarrier}$ represent the weight of the entrapped drug and the total weight of the corresponding drug-entrapped NPs, respectively.

2.7 | In vitro release of Baicalein

The release behavior of Ba from all formulations (BSA-Ba NPs, BSA-Ba@Zn NPs, and BSA-Ba@Zn–Glu NPs) was evaluated by using the sample and separate (SS) method.[26] All purified and freeze-dried formulations (without free Ba) were dispersed in 1.5 ml of PBS, pH 7.4 and pH 5.5, and kept at 37°C (120 rpm). At arranged time intervals, the samples were centrifuged, and the supernatant was withdrawn to determine the Ba release amount by UV–Vis spectrophotometer. The sink condition was maintained by replacing it with an equal amount of fresh buffer after each withdrawal.

2.8 | Drug release kinetic estimation

To study release mechanism and kinetic, the in vitro Ba release records were analyzed by fitting them to different kinetic models, as shown in Table S1. The best kinetic model was designated based on the lowest values for the mean squared error (MSE) and Akaike's information criterion (AIC).

2.9 | Hemocompatibility assay

Hemolysis of red blood cells (RBCs) refers to the breakdown of the RBC membrane, which results in the release of hemoglobin into the blood plasma. As a result, the hemolytic degree of all formulations must be justified to support their biocompatibility, which was assessed using a previously reported approach.[23] The percentage of hemolysis was estimated using the formula:

$$Hemolysis(\%) = \frac{A_{treated\ sample} - A_{negative\ control}}{A_{positive\ control} - A_{negative\ control}} \times 100$$

2.10 | Cell viability assay

U87 cells were cultured in DMEM medium supplemented with 10% FBS at 37°C in a humidified atmosphere with 5% CO_2. MTT assays were used to evaluate the effect of the prepared NPs on U87 cell viability. U87 cells (1.2×10^4 cells) were seeded in 96-well plates and treated with different concentrations (5–30 μM) of the samples (Zn NPs, BSA NPs, BSA@Zn NPs, BSA@Zn-Glu NPs, Free Ba, BSA-Ba NPs, BSA-Ba@Zn NPs, and BSA-Ba@Zn-Glu NPs) after achieving 70%–80% confluency. Twenty four hours after treatment, each well was supplied with 20 μl of MTT solution (5 mg ml^{-1}) and incubated for 3 h at 37°C with 5% CO_2. Next, the MTT solution was removed, and formazan crystals were dissolved in DMSO (150 μl/well). Finally, the absorbance of each well was measured at 570 nm in a microplate reader.

2.11 | Apoptosis assay

Apoptosis assay was performed with 10 μM for 24 h post-treatment to determine the effects of free Ba, BSA-Ba@Zn NPs, BSA@Zn-Glu NPs, and BSA-Ba@Zn-Glu NPs on apoptosis of U87 cells. After treatment, the cells were collected and washed; the pellet was dissolved in 100 μl of annexin V binding buffer and stained with annexin V-FITC (Biolegend) and propidium iodide (PI) (Sigma-Aldrich) under the manufacturer's protocol. Data acquisition and analysis were conducted via flow cytometry and FlowJo software (Tree Star, Ashland, OR).

3 | RESULTS

3.1 | FT-IR

Figure 1a compares the FT-IR spectra of BSA NPs, Zn NPs, and BSA@Zn NPs to confirm the practical synthesis of BSA@Zn NPs. The prominent transmittance peaks in the FT-IR spectrum of BSA NPs were the BSA C—H vibration band at 2960 cm^{-1}, the amide I band (C═O stretching) at 1700–1600 cm^{-1}, and the amide II band (C—N stretching and bending of the N—H band) at 1450 and 1550 cm^{-1}.[27] The FT-IR spectrum of BSA@Zn NPs shows the peaks shift toward a higher wavelength with lower peak intensity, which was assumed to be due to the interaction of BSA with Zn NPs. Also, The FT-IR spectrum of Zn NPs revealed several absorption bands in the spectrum of BSA@Zn NPs. This observation strongly supported that the Zn NPs were successfully hybridized into the BSA NP matrix.

Figure 1b shows the FT-IR spectra of free Ba, BSA-Ba NPs, and BSA NPs. The Ba spectrum exhibits characteristic peaks at 3408.6 cm^{-1} (O—H stretching vibration), 1657.7 cm^{-1} (C═O stretching vibration), and 1390 cm^{-1} (O—H bending vibration).[28,29] Moreover, compared with FT-IR spectra of BSA NPs, there are some transmittance peaks that appeared at 1257 and 1390 cm^{-1} in BSA-Ba. It may be suggested that the free Ba was successfully loaded into BSA NPs and produced the BSA-Ba NP formulation. Likewise, characteristic peaks for free Ba were distinguished in the FT-IR spectrum of the BSA-Ba@Zn NPs,

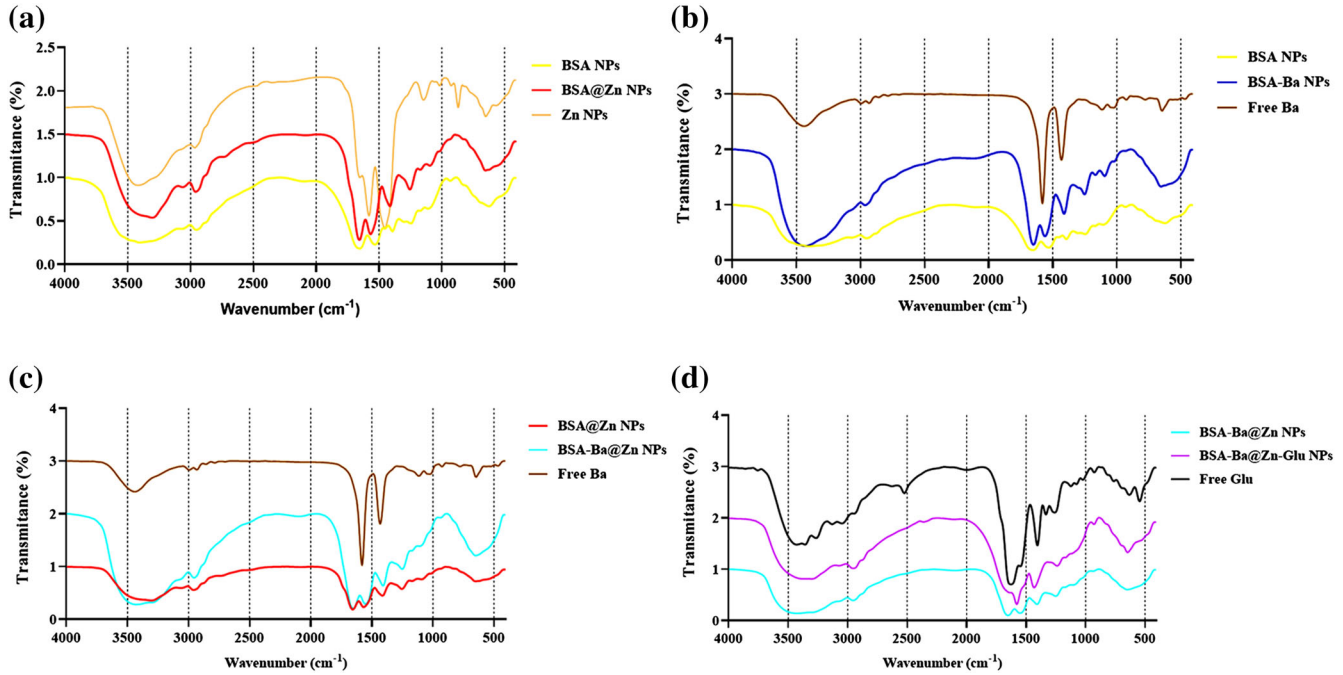

FIGURE 1 Fourier transform infrared spectroscopy (FT-IR). (a) FT-IR spectra of Zn nanoparticles (NPs), bovine serum albumin (BSA) NPs, and BSA@Zn NPs. (b) FT-IR spectra of BSA NPs, Baicalein-loaded BSA NPs (BSA-Ba NPs), and free Ba. (c) FT-IR spectra of BSA@Zn NPs, Zn NPs hybridized with BSA-Ba NPs (BSA-Ba@Zn NPs), and free Ba. (d) FT-IR spectra of BSA-Ba@Zn NPs, Glu-conjugated BSA-Ba@Zn NPs (BSA-Ba@Zn-Glu NPs), and free Glu

which also illustrates that the formation was successfully synthesized (Figure 1c).

In Figure 1d, the spectrum of glutamate (Glu) shows several characteristic peaks at 3490, 2850, 1690, and 1476 cm^{-1}, which are attributed to O—H stretching vibration, C—H stretching vibration, and carbonyl stretching, and N—H amino group stretching, respectively. All spectrum peaks of the BSA-Ba@Zn NPs appeared in the spectrum peaks of BSA-Ba@Zn-Glu NPs, whereas the peak of the carbonyl group function (1690 cm^{-1}) had not appeared. This observation suggested that the final formulation (BSA-Ba@Zn-Glu NPs) was successfully synthesized.

3.2 | Particle size and morphology

The average hydrodynamic diameter and *zeta* potential for the nanostructures are presented in Figure 2a–d. The average hydrodynamic size of all formulations was 142.40 ± 1.91 to 177.10 ± 1.87 nm (mean ± SD). The average *zeta* potential of NPs before using glutamate (BSA NPs, Zn NPs, BSA@Zn NPs, BSA-Ba NPs, and BSA-Ba@Zn NPs) was −10.57 ± 0.71 to −32.00 ± 2.96 mV (mean ± SD) and after using glutamate (BSA@Zn-Glu and BSA-Ba@Zn-Glu nanostructures) was −34.23 ± 0.35 to −35.77 ± 0.60 mV. BSA NPs are significantly different in comparison to other formulations in terms of size and *zeta* potential, as can be seen in Figure 3a. In addition, the PDI for all formulations was 0.133 to 0.447, which indicated that NPs have normal size distribution. Uniform distribution and good spherical morphology of the final formulation (BSA-Ba@Zn-Glu NPs) were confirmed by FESEM techniques (Figure 3b).

3.3 | Baicalein release behavior and kinetics

Drug loading amounts of various Ba-loaded nanoparticle formulations (BSA-Ba NPs, BSA-Ba@Zn NPs, and BSA-Ba@Zn-Glu NPs) were found at 25.32% ± 3.87%, 18.92% ± 2.46%, and 17.48 ± 1.93%, respectively. The in vitro Ba release from the Ba-loaded NPs (BSA-Ba NPs, BSA-Ba@Zn NPs, and BSA-Ba@Zn-Glu NPs) was carried out at 37°C using PBS in pH values of 7.4 and 5.5. Different pH values were used to simulate the drug release of pH-sensitive nanostructure in normal and tumor tissue conditions. The release behavior of synthesized nanostructure is shown in Figure 4a,b, which observed an initial minor burst release during the first 2 h (pH 7.4 & 5.5). This is followed by sustained and controlled release between 3 and 72 h, and a plateau phase was reached after 96 h (Table 1).

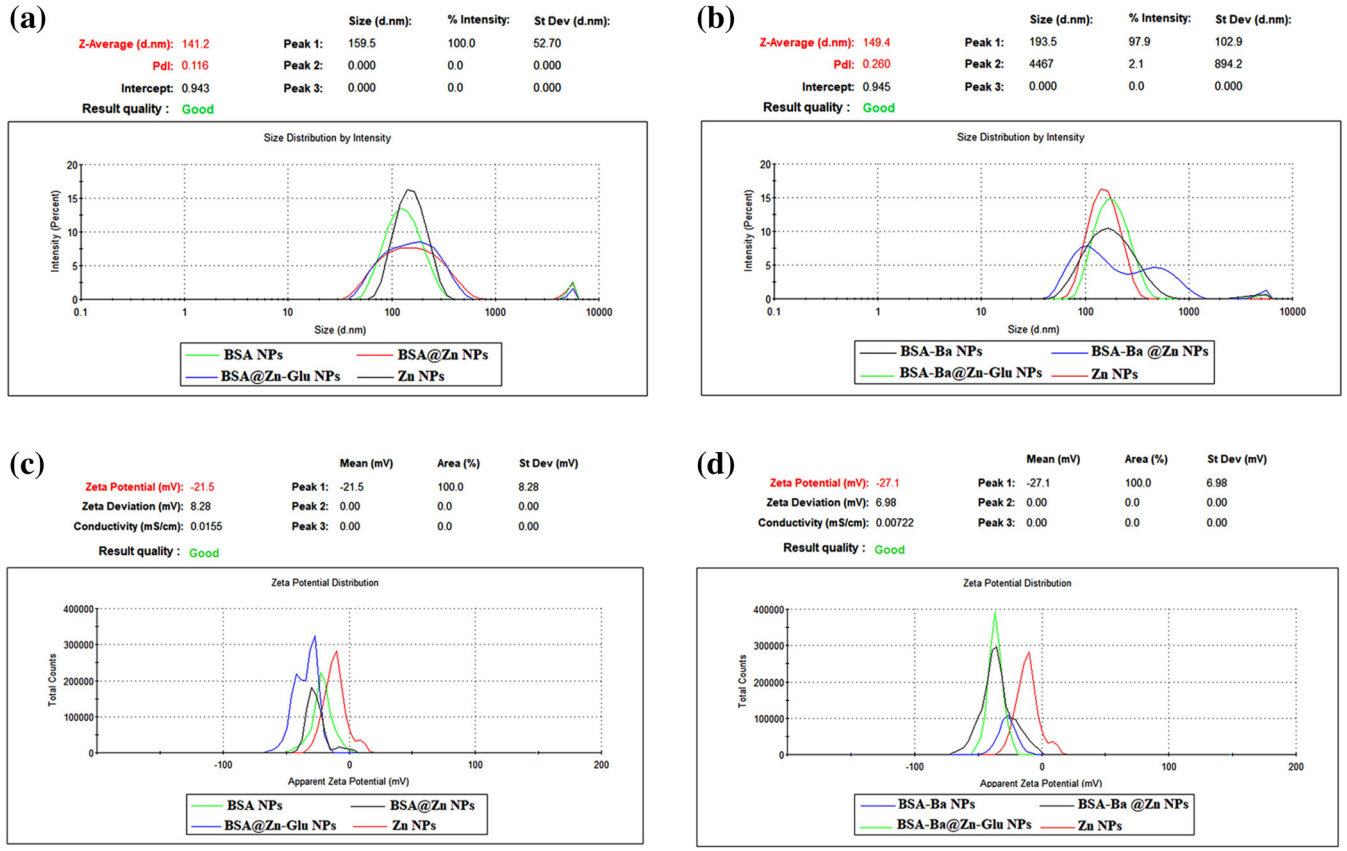

FIGURE 2 Dynamic light scattering (DLS) analysis under optimal conditions. (a, b) Hydrodynamic diameters (average hydrodynamic diameter [Z-average; nm]) of nanostructure systems. (c, d) *Zeta* potential (mV) of nanostructure systems by DLS. BSA NPs, bovine serum albumin nanoparticles; BSA-Ba NPs, Baicalein-loaded BSA NPs; BSA-Ba@Zn NPs, Zn NPs hybridized with BSA-Ba NPs; BSA-Ba@Zn-Glu NPs, Glu-conjugated BSA-Ba@Zn NPs

As shown in Table 2, the results from empirical Ba release data were fitted with different mathematical kinetic models. As indicated, the R^2, AIC, and MSE values of the Makoid–Banakar showed the most fitness with the experimental data in BSA-Ba NPs and BSA-Ba@Zn NPs at pH 7.4 media as well as BSA-Ba@Zn-Glu NPs in both pH media (pH 7.4 and 5.5), whereas Gompertz model was the best model with experimental data for BSA@Ba NPs and BSA-Ba@Zn NPs at pH 5.5 based on the R^2, AIC, and MSE values.

3.4 | BSA-Ba@Zn-Glu NP hemocompatibility

The purified RBC samples were incubated with various concentrations of prepared NPs (BSA NPs, BSA@Zn NPs, BSA@Zn-Glu NPs, BSA-Ba NPs, BSA-Ba@Zn NPs, BSA-Ba@Zn-Glu NPs, and Zn NPs) from 1 to 8 mg ml^{-1}. As shown in Figure 5a, the hemolytic activity of nanostructures ranged from 4.24% ± 0.32% to 11.49% ± 0.43%.

3.5 | BSA-Ba@Zn-Glu NPs reduce cell viability

The U87 cell proliferation was repressed by all treatments of Free Ba, BSA-Ba NPs, BSA-Ba@Zn NPs, and BSA-Ba@Zn-Glu NPs compared with the control after 24 h treatment. The maximum inhibition was detected at 30 μM. The obtained results indicate that Zn NPs (concentration of 10 and 30 with $^{****}p < 0.0001$), BSA NPs (concentration of 30 with $^{****}p < 0.0001$), and BSA@Zn NPs (concentration of 10 with $^{*}p < 0.05$) inhibit the growth of U87 cells compared with the control group (Figure 5b). The BSA@Zn-Glu NPs did not significantly inhibit the growth of these cells compared with the control at each investigated concentration at 24 h post-treatment, which may be related to the decrease of nanostructure toxicity by adding glutamate amino acid.

Present results revealed that BSA-Ba@Zn-Glu NPs inhibit U87 cell growth more than BSA-Ba@Zn NPs, indicating more uptake of BSA-Ba@Zn-Glu

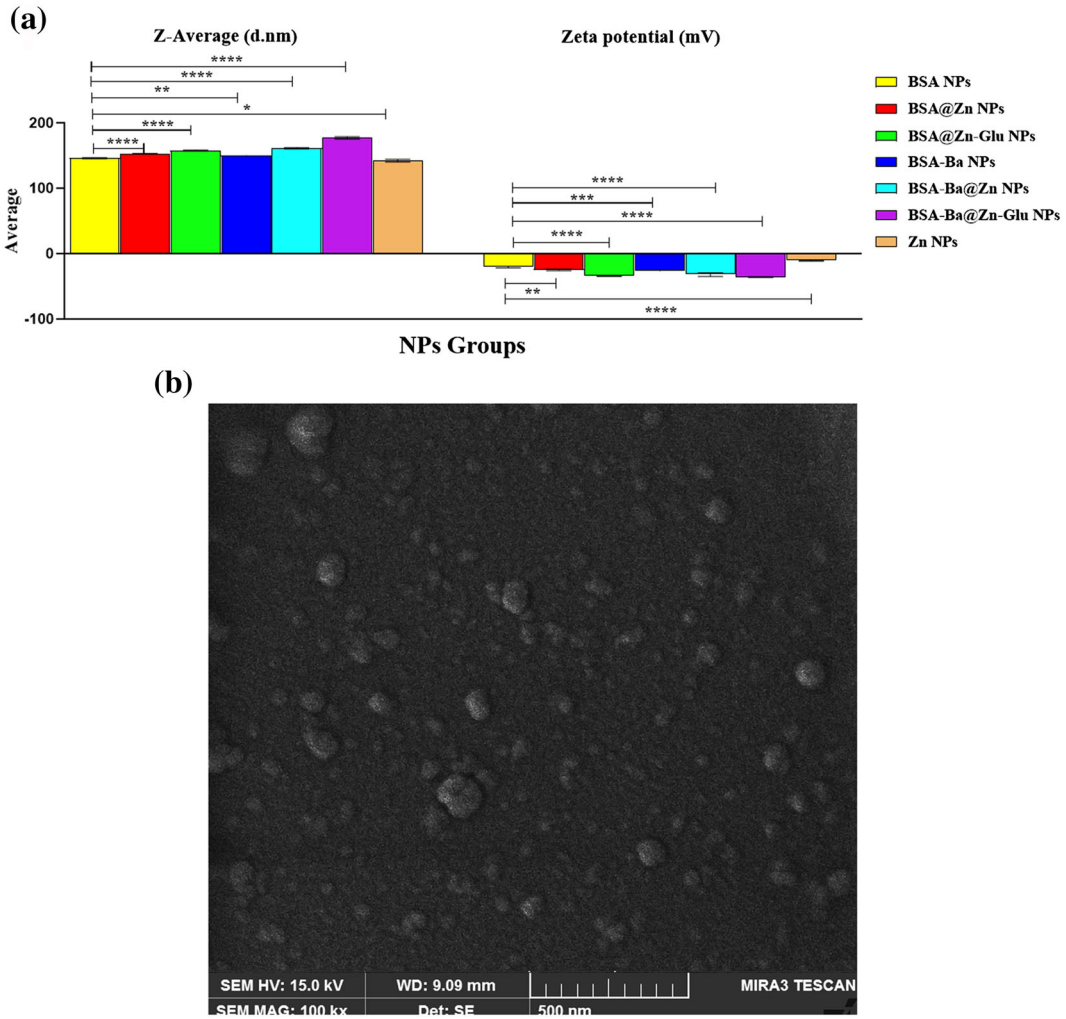

FIGURE 3 Size, *zeta* potential, and morphology analysis. (a) Average hydrodynamic diameter (Z-average) (nm) and *zeta* potential average (mV) of synthesized nanostructure. (b) Field emission scanning electron microscopy (FESEM) analysis of synthesized nanostructure. BSA NPs, bovine serum albumin nanoparticles; BSA-Ba NPs, Baicalein-loaded BSA NPs; BSA-Ba@Zn NPs, Zn NPs hybridized with BSA-Ba NPs; BSA-Ba@Zn-Glu NPs, Glu-conjugated BSA-Ba@Zn NPs. Data are expressed as the mean ± SD of three independent experiments; $^{*}P < 0.05$, $^{**}P < 0.01$, $^{***}P < 0.001$, and $^{****}P < 0.0001$.

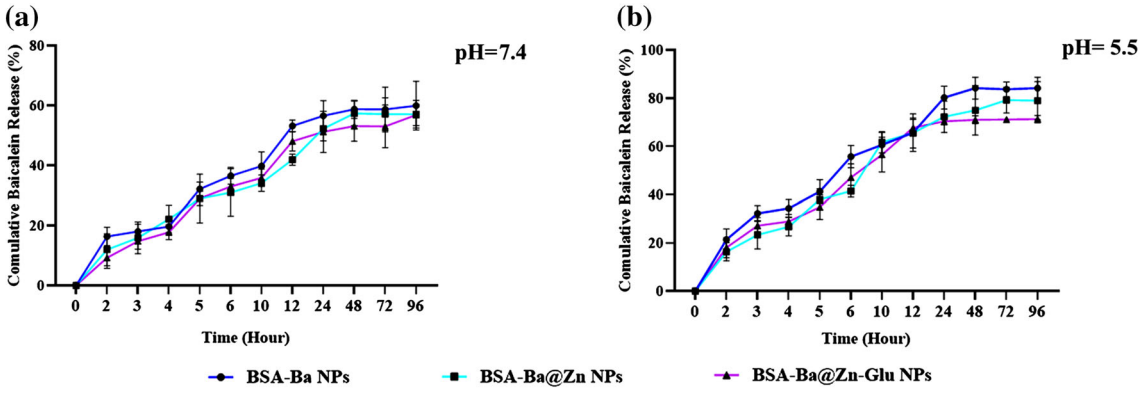

FIGURE 4 In vitro release assay. Accumulative Baicalein release profile of the nanostructures at (a) pH = 7.4 and (b) pH = 5.5. BSA-Ba NPs, Baicalein-loaded BSA NPs; BSA-Ba@Zn NPs, Zn NPs hybridized with BSA-Ba NPs; BSA-Ba@Zn-Glu NPs, Glu-conjugated BSA-Ba@Zn NPs

TABLE 1 Release profile parameters of the formulations

Formulation	pH	Ba release after 2 h (%)	Cumulative Ba release after 24 h (%)	Maximum Ba depletion (%)	Release rate (%/h)
BSA-Ba NPs	7.4	16.385 ± 3.019	56.588 ± 5.102	59.988 ± 8.153	0.45
	5.5	21.350 ± 4.455	80.276 ± 4.719	84.213 ± 4.480	0.56
BSA-Ba@Zn NPs	7.4	11.946 ± 5.350	52.288 ± 4.142	57.094 ± 4.614	0.44
	5.5	16.333 ± 3.772	72.258 ± 6.496	78.958 ± 7.905	0.57
BSA-Ba@Zn-Glu NPs	7.4	9.255 ± 3.483	51.246 ± 6.885	56.876 ± 3.542	0.45
	5.5	18.038 ± 4.119	70.412 ± 1.506	71.321 ± 1.542	0.47

Abbreviations: BSA-Ba NPs, Baicalein-loaded BSA NPs; BSA-Ba@Zn NPs, Zn NPs hybridized with BSA-Ba NPs; BSA-Ba@Zn-Glu NPs, Glu-conjugated BSA-Ba@Zn NPs.

nanostructure into cells due to the high expression of glutamate receptor (AMPA) on the U87 cell. Also, obtained results showed that BSA-Ba@Zn-Glu NPs inhibited cell growth more than BSA@Zn-Glu NPs in a dose-dependent manner. It revealed that the effect of Ba reduces the viability of U87 cells.

3.6 | BSA-Ba@Zn-Glu NPs induce apoptosis in U87 cells

The results showed that BSA-Ba@Zn-Glu NPs (****$p < 0.0001$), free Ba, BSA-Ba@Zn NPs (***$p < 0.001$), and BSA@Zn-Glu NPs (*$p < 0.05$) treatment caused a statistically higher total apoptotic rate (early and late apoptosis) in comparison with the control after 24 h incubation. Treatment of cells with 10 μM BSA-Ba@Zn-Glu NPs could significantly increase total apoptosis in U87 cells compared with free Ba, BSA-Ba@Zn NPs, and BSA@Zn-Glu NPs (Figure 6).

4 | DISCUSSION

Cancer is usually treated by surgery, chemotherapy, and radiotherapy as conventional therapies. In spite of the efficacy of these methods, in theory, their nonselective properties could cause a lot of critical side effects.[30,31] Recently, the application of nanosystems, with easy surface functionalization, high biocompatibility, drug delivery capacity, and cancer targeting, has shown the potential to reduce these side effects. Among these particles, zinc nanoparticles are considered safe in both conditions (in vitro and in vivo). Due to their highly biocompatible and biodegradable features, they could be considered potent nano-platforms for cancer treatment.[32–34]

Generally, the green synthesis way of the metallic nanoparticles provides advancements over chemical methods as it is environment friendly, cost-effective, and easily scaled up for large-scale synthesis.[11,35] Also, numerous studies described BSA as an appropriate component for succeeding biocompatible nanoparticles or nanostructures. It suggested that the BSA NPs developed via Zn NPs have several advantages, including antibacterial, anticancer, immunomodulatory, sunscreen, and antioxidant effects. On the other hand, they may be used as an adjuvant treatment to chemotherapeutic drugs to alleviate their toxic effects.[36–38] In the present study, all formulations were prepared based on BSA and successfully hybridized with Zn NPs according to our previously reported method.[24] The natural active compound, Ba, was used as a potential anticancer therapeutic agent.

Herein, the Zn NPs were fabricated based on green synthesis techniques that we introduced as a fast and facile synthesis method over conventional strategies.[39] BSA was used as a reducing agent to prepare the Zn NPs. BSA functional groups, including amine (—NH_2), the carboxylic acid (—COOH), hydroxyl (—OH), and thiol (—SH) groups, can act as active binding sites (covalent or noncovalent) for multiple therapeutic agents. BSA is a single chain of polypeptides consisting of 583 residual amino acids with a molecular weight of 66 kDa. Several studies have reported that albumin may interact as a ligand with cellular receptors including glycoproteins Gp60, Gp30, and Gp18, secreted protein acidic and rich in cysteine (SPARC), megaline/cobilin complex, and neonatal Fc receptors (FcRn).[40–45] The tertiary structure of BSA contains multiple cysteine residues forming 17 disulfide bonds to produce pattern-specific folding.[46] The protein is thermally unfolded when heated at 90°C, resulting in further promotion to break off the disulfide bonds and then the formation of more —SH groups. Both —SH and hydroxyl groups in the unfolded structure of BSA could be possessed a reduction of aqueous zinc ions [Zn (II)) to metallic zinc (Zn (0)] and result in a color change from colorless to a very bright and clear yellow color. Furthermore, the synthesized NPs can be conjugated by Glu

TABLE 2 R^2, Akaike's information criterion (AIC), and mean squared error (MSE) parameters from fitting release data of formulations on various models

Formulation	BSA-Ba NPs						BSA-Ba@Zn NPs						BSA-Ba@Zn-Glu NPs					
pH	7.4			5.5			7.4			5.5			7.4			5.5		
Model	R^2	MSE	AIC	R^2	MSE	AIC	R^2	MSE	AIC	R^2	MSE	AIC	R^2	MSE	AIC	R^2	MSE	AIC
Zero order	0.6058	671.10	108.89	0.7339	1353.13	117.29	0.3199	498.99	105.32	0.4416	1081.17	114.60	0.3787	523.37	105.90	0.8514	1133.82	115.17
First order	0.6129	178.10	93.82	0.8786	94.85	85.39	0.2297	291.22	98.86	0.7990	105.73	90.96	0.1194	334.29	100.52	0.5931	249.18	96.99
Higuchi	0.6388	166.18	92.98	0.5179	376.24	101.94	0.6878	118.02	88.02	0.6039	297.06	99.10	0.6140	146.54	90.62	0.4182	356.30	101.28
Korsmeyer–Peppas	0.8623	63.34	81.41	0.8963	89.04	85.50	0.9113	36.88	74.92	0.8658	110.75	88.12	0.8522	61.71	81.10	0.8373	109.63	87.99
Hixson–Crowell	0.1545	482.92	104.93	0.5138	379.40	104.04	0.0413	362.43	101.49	0.5600	329.97	100.36	0.0571	401.29	102.71	0.2758	443.50	103.91
Hopfenberg	0.1028	412.82	103.91	0.8786	104.25	87.39	0.2295	320.41	100.87	0.7990	165.85	92.96	0.1190	367.89	102.52	0.5930	274.15	98.99
Baker–Lonsdale	0.7078	122.23	88.45	0.8631	106.80	86.83	0.8104	71.68	82.04	0.8394	120.48	88.27	0.7352	100.51	86.10	0.7093	178.05	92.96
Makoid–Banakar	**0.9492**	**25.96**	**71.45**	0.9742	24.62	70.81	**0.9820**	**8.31**	**57.78**	0.9521	43.93	77.76	**0.9343**	**30.48**	**73.37**	**0.9472**	**39.480**	**76.48**
Peppas–Sahlin	0.9438	28.74	72.67	0.9714	27.32	72.06	0.9793	9.54	59.44	0.9461	49.39	79.16	0.9277	33.56	74.53	0.9391	45.55	78.19
Weibull	0.9227	39.54	76.50	0.9728	25.90	71.42	0.9665	15.48	65.24	0.9516	44.04	77.89	0.9319	31.62	73.81	0.9247	56.37	80.75
Quadratic	0.4102	271.39	98.77	0.3702	540.62	107.14	0.5847	172.72	93.45	0.4822	427.15	104.32	0.4804	216.98	96.19	0.2972	473.44	105.55
Logistic	0.9044	43.97	77.03	0.9737	22.58	69.03	0.9472	21.95	68.70	94.69	43.82	76.99	0.8918	45.16	77.35	0.9068	62.81	81.31
Gompertz	0.9259	34.10	73.98	**0.9826**	**14.96**	**64.09**	0.9658	14.21	63.47	**0.9664**	**27.75**	**71.51**	0.9184	34.05	73.97	0.9297	47.36	77.92
Probit	0.9069	42.82	76.71	0.9694	26.24	70.84	0.9506	20.56	67.91	0.9432	46.87	77.80	0.8970	43.00	76.76	0.9041	64.60	81.65

Note: These numbers shown in bold are actually the optimal numbers related to our prepared NPs formulation.

Abbreviations: BSA-Ba NPs, Baicalein-loaded BSA NPs; BSA-Ba@Zn NPs, Zn NPs hybridized with BSA-Ba NPs; BSA-Ba@Zn-Glu NPs, Glu-conjugated BSA-Ba@Zn NPs.

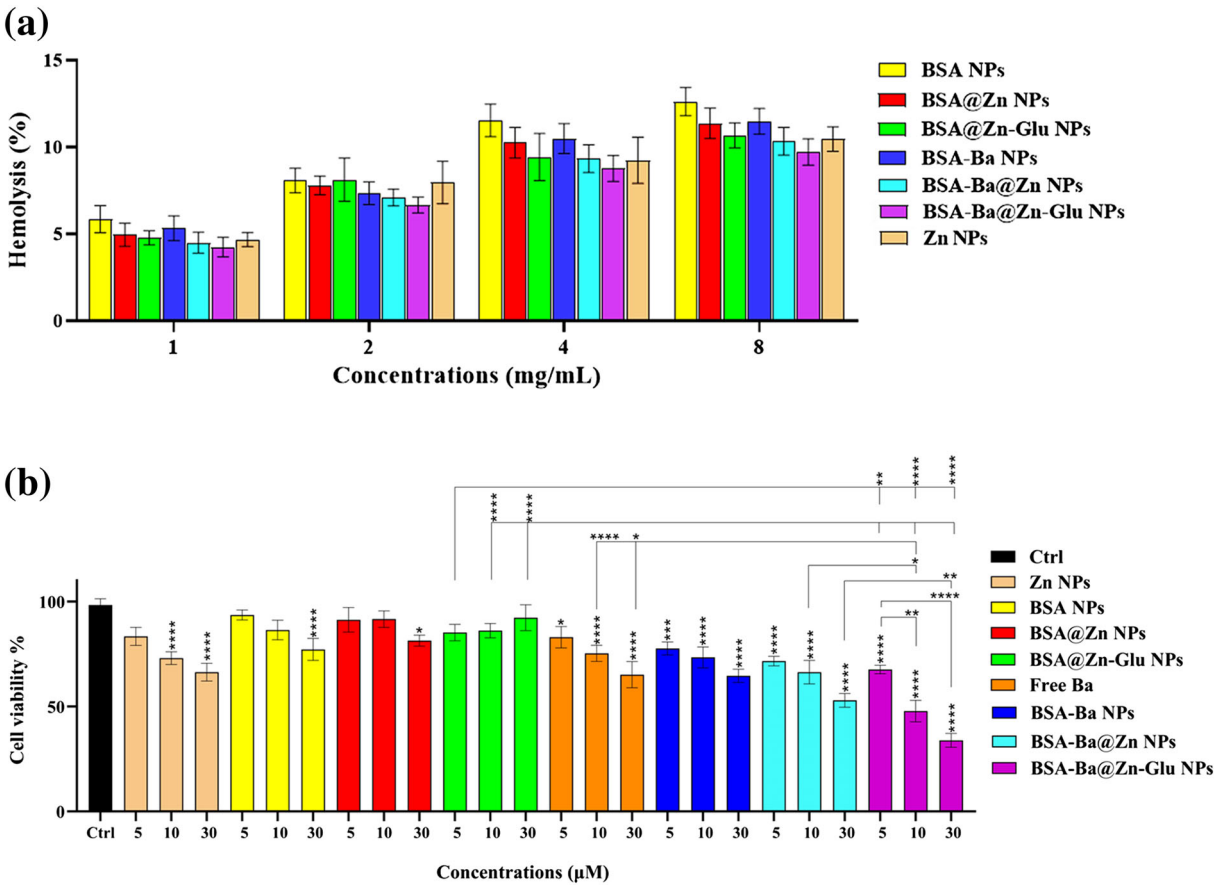

FIGURE 5 Percentage of hemolysis induction (a) and cell viability inhibition (b) after treatment with various concentrations of nanoparticles (NPs). Values with *$p < 0.05$, **$p < 0.01$, ***$p < 0.001$, and ****$p < 0.0001$ were regarded as statistically meaningful. BSA NPs, bovine serum albumin nanoparticles; BSA-Ba NPs, Baicalein-loaded BSA NPs; BSA-Ba@Zn NPs, Zn NPs hybridized with BSA-Ba NPs; BSA-Ba@Zn-Glu NPs, Glu-conjugated BSA-Ba@Zn NPs

(BSA@Zn-Glu NPs & BSA-Ba@Zn-Glu NPs) to increase the efficiency of the designed nanostructures. The biological rationale for using Glu is their presumed effect on the interaction with metabotropic glutamate receptors (mGluR) to mediate intracellularly, resulting in an inhibition of U87 cell growth, as shown in our results.[47]

The generation of versatile systems with a specific size and morphological form shows a significant role in the development of modern drug delivery systems and their clinical applications.[47] BSA, zinc sulfate, Ba, and Glu were used to design and synthesize the suggested nanostructures. BSA was used as a reducing agent to prepare the Zn NPs and also as a nanostructure system to develop the final formulation. All elements such as temperature, stirring time, amounts of acetone, and high- or low-speed addition of acetone were critical factors during the nanostructure synthesis process, which is a crucial role in obtaining small NPs with a low PDI, as previously reported.[48] The successful synthesis of all NP samples can be confirmed by FT-IR spectroscopy. Our results obtained from the FT-IR spectra of the BSA NPs, Zn NPs, Ba, and Glu are similar to the results reported by previous studies in other aspects.[27,49–53] Peak shifts in BSA@Zn NPs suggested that BSA had a strong interaction with the Zn, due to the coordination of Zn^{2+} with the C═O, —NH, and —OH groups of BSA. Also, FT-IR spectra of Baicalein and glutathione were consistent with previous studies.[50,54] Glutathione increases the stability of the synthesized nanoparticles by increasing the negative charge of their surface, thus reducing the aggregation of nanoparticles.

All of the formulations had a negative *zeta* potential, which could be due to the hydroxyl groups in BSA. Furthermore, the *zeta* potential values of the BSA@Zn-Glu NPs and BSA-Ba@Zn-Glu NPs were significantly higher *zeta* potential values related to the negatively charged Glu molecules in formulations. Due to electrostatic forces between the obtained nanoparticles, the very negative *zeta* potential values may provide excellent physical stability in water.

The release profile was defined by considering three major factors: burst release, maximal Ba depletion

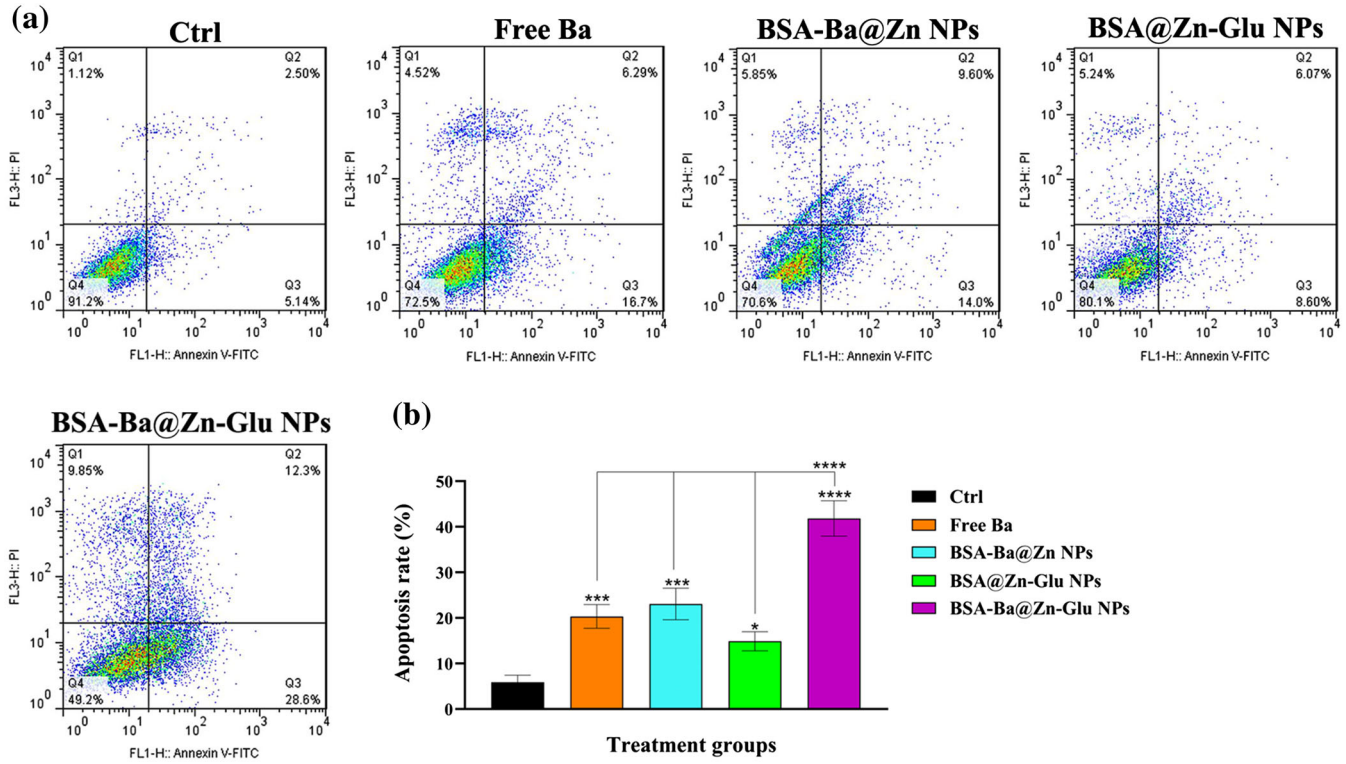

FIGURE 6 Treatment effects of nanostructure loaded with Ba on apoptosis of U87 cells. (a) Cells were incubated with optimum (as control), free Ba, BSA-Ba@Zn NPs, BSA@Zn-Glu NPs, and BSA-Ba@Zn-Glu NPs at 10 μM concentration for 24 h, and apoptosis was examined using annexin V-FITC/propidium iodide (PI) staining and flow cytometry analysis. One representative flow cytometry analysis of apoptosis in U87 cells is shown; fluorescence intensity for annexin V/FITC is plotted on the x-axis, and PI is plotted on the y-axis (Q1, necrosis; Q2, late apoptosis; Q3, early apoptosis; and Q4, live cells). (b) Statistical analysis of variance of apoptotic cell percentage for all samples. Value with $^{*}p < 0.05$, $^{***}p < 0.001$ and $^{****}p < 0.0001$was regarded as statistically meaningful. BSA-Ba@Zn NPs, Zn NPs hybridized with BSA-Ba NPs; BSA-Ba@Zn-Glu NPs, Glu-conjugated BSA-Ba@Zn NPs

quantity (MBDQ), and release rate (Table 1). The total cumulative Ba released after 2 h was characterized as the burst release. The nanostructure system was categorized as a low burst release. The amount of Baicalein on the nanostructure system's surface has been related to the quantity of burst release.[55] As a result, the lower the burst release, the lower the Ba on the nanostructure surfaces. The second factor was the MBDQ, which nanostructure system based on the BSA NPs could retain a high amount of Ba inside themselves.[56] The third characteristic of release profiles is the rate of release. The rate of Ba release from the starting point of the ascending part of the profile to reach the plateau was calculated. As shown in Table 1, there is no significant difference in the release rate between pH media. Furthermore, the nanostructure systems are fitted by nonlinear Gompertz and Weibull models.[57,58]

The results of the hemocompatibility assay demonstrated that no significant hemolytic activity was observed in the nanostructure systems, confirming that the mentioned systems have adequate biocompatibility. In medical applications, the toxicity of nanostructure systems is a crucial concern. Previously, it has been indicated that low and high zinc concentrations on cells initiate cancer progression and pose toxic effects, respectively. The probable mechanism of this cytotoxic effect could be due to oxidative stress via reactive oxygen species (ROS).[59] In the present study, BSA NPs, BSA@Zn NPs, and BSA@Zn-Glu NPs have no significant in vitro cytotoxic effects in the lower concentrations. Obtained results demonstrated that the cytotoxicity of the ZnNPs was reduced when hybridized by BSA NPs (e.g., BSA@Zn NPs), and it was further reduced by conjugated with glutamate amino acid.[60,61] On the other hand, BSA-Ba@Zn-Glu NPs in all used concentrations reduce the cell viability of U87 cells in a dose-dependent manner in the current study. These data also suggested that the cell growth inhibition effect of BSA-Ba@Zn-Glu was due to the Baicalein in the nanostructure system because BSA@Zn-Glu did not show a significant cytotoxicity effect in vitro.

Previous studies on Baicalein (Ba) report anticancer effects via proliferation inhibition and apoptosis induction in human GBM U251 cells.[62] Liu et al. have

reported that Baicalein induces autophagy and apoptosis via the AMPK pathway.[63] Another study has reported that reduction of C6 and U87 cell viability occurs by Baicalein exposure. Baicalein treatment of U87 cells could increase apoptotic cell percentage and lead to the release of cytochrome c from mitochondria.[64] In the present study, the cytotoxicity rate of BSA-Ba@Zn-Glu nanoparticles with low loading of Baicalein was more compared with pure drug (free drug 10 μM). Furthermore, BSA-Ba@Zn-Glu NPs were more involved in reducing cell viability than BSA-Ba@Zn, which could be related to the increased cellular uptake of BSA-Ba@Zn-Glu NPs by glutamate AMPA receptors on U87 cancer cells. Previously, the cytotoxic effect of Zinc nanoparticles on glioma cancer cells such as A172, U87, A172, U87, LNZ308, LN18, LN229, and breast, and prostate cancer cells, along with normal cells has been studied. It has been reported that Zinc nanoparticles have cytotoxic effects on cancer cells while posing no cytotoxic effect on normal cells. Zinc nanoparticles have been shown to cause less influence on ROS production in normal astrocytes.[65]

It has been reported that loss in the balance of protein activities leads to increased levels of ROS resulting in apoptosis death. Accordingly, Zinc nanoparticles present cytotoxicity in cancer cells due to elevated intracellular levels of dissolved zinc ions, followed by increased ROS production, which causes cancer cell death.[66] Our result showed that the BSA-Ba@Zn-Glu NPs could significantly induce apoptosis in the U87 cancer cells compared with other groups (free Ba, BSA-Ba@Zn, and BSA@Zn-Glu NPs). The apoptosis rate by BSA@Zn-Glu NPs was not much due to the coating of nanoparticles with glutamate and reducing their toxicity. Overall, these results suggest that the final formulation (BSA-Ba@Zn-Glu NPs) provides promising strategies for reducing cell proliferation and inducing cell apoptosis.

5 | CONCLUSION

In this study, Zn NPs were synthesized based on a green synthesis method. BSA NPs were used as a nano-platform for Glu conjugation and Ba drug delivery. At the same time, BSA was utilized as a reducing agent for the green synthesis of Zn NPs, which hybridized with BSA NPs to form BSA-Ba@Zn-Glu NPs as a suggested nanosystem. Our study showed that BSA-Ba@Zn-Glu NPs induce cytotoxicity and apoptosis in human brain cancer cells (U87) in a dose-dependent manner. It can be concluded that Zn NPs and Baicalein have synergistic effects in reducing the survival of U87 cancer cells, and consequently, the presented nanostructure can be a promising tool for targeted drug delivery and multifunctional biomedicine applications.

ACKNOWLEDGMENTS

The authors would like to thank the staff of the Medical Biotechnology Department of Zanjan University of Medical Sciences and pharmaceutical lab for their technical assistance.

AUTHOR CONTRIBUTIONS

Mahmoud Gharbavi: Methodology, conceptualization, software, writing — original draft, and editing. **Behrooz Johari**: Supervision, project administration, writing — review and editing, and final approval. **Roghayeh Ghorbani**: Methodology. **Hamid Madanchi**: Methodology. **Ali Sharafi**: Supervision and editing.

CONFLICT OF INTEREST

The grant was received by Behrooz Johari from Zanjan University of Medical Sciences. All the authors declare no financial or commercial conflict of interest that could negatively influence the study.

DATA AVAILABILITY STATEMENT

The data sets used and/or analyzed during the current study are available from the corresponding author on reasonable request.

ORCID

Mahmoud Gharbavi https://orcid.org/0000-0002-9580-1999
Behrooz Johari https://orcid.org/0000-0003-3440-572X
Ali Sharafi https://orcid.org/0000-0002-6012-1424

REFERENCES

[1] Q. Ostrum, H. Gittleman, J. Fulop, M. Liu, R. Blanda, C. Kromer, Y. Wolinsky, C. Kruchko, J. S. Barnholtz-Sloan, *Neuro Oncol.* **2015**, *17*(suppl 4), v1.
[2] H. Ohgaki, *Cancer Epidemiol.* **2009**, 323.
[3] P. Y. Wen, S. Kesari, *N. Engl. J. Med.* **2008**, *359*(5), 492.
[4] R. Altieri, F. Zenga, M. M. Fontanella, F. Cofano, A. Agnoletti, G. Spena, E. Crobeddu, R. Fornaro, A. Ducati, D. Garbossa, *Surg. Technol. Int.* **2015**, *27*, 297.
[5] D. Friedmann-Morvinski, *Crit. Rev. Oncog.* **2014**, *19*(5), 327.
[6] S. Al-Musawi, S. Ibraheem, S. Abdul Mahdi, S. Albukhaty, A. J. Haider, A. A. Kadhim, K. A. Kadhim, H. A. Kadhim, H. Al-Karagoly, *Life* **2021**, *11*(1), 71.
[7] W. M. Pardridge, *Pharm. Res.* **2007**, *24*(9), 1733.
[8] X. Guo, L. Huang, *Acc. Chem. Res.* **2012**, *45*(7), 971.
[9] W. Lohcharoenkal, L. Wang, Y. C. Chen, Y. Rojanasakul, *Biomed. Res. Int.* **2014**, *2014*, 1, 180549.
[10] I. H. Shah, M. Ashraf, I. A. Sabir, M. A. Manzoor, M. S. Malik, S. Gulzar, F. Ashraf, J. Iqbal, Q. Niu, Y. Zhang, *J. Mol. Struct.* **2022**, *1259*, 132696.

[11] B. A. Abbasi, J. Iqbal, Z. Khan, R. Ahmad, S. Uddin, A. Shahbaz, S. A. Zahra, M. Shaukat, F. Kiran, S. Kanwal, T. Mahmood, *Microsc. Res. Tech.* **2021**, *84*(2), 192.
[12] J. W. Rasmussen, E. Martinez, P. Louka, D. G. Wingett, *Expert Opin. Drug Deliv.* **2010**, *7*(9), 1063.
[13] S. S. Willard, S. Koochekpour, *Int. J. Biol. Sci.* **2013**, *9*(9), 948.
[14] M. C. Oh, J. M. Kim, M. Safaee, G. Kaur, M. Z. Sun, R. Kaur, A. Celli, T. M. Mauro, A. T. Parsa, *PLoS One* **2012**, *7*, e47846.
[15] S. Chikara, L. D. Nagaprashantha, J. Singhal, D. Horne, S. Awasthi, S. S. Singhal, *Cancer Lett.* **2018**, *413*, 122.
[16] S. Singh, B. Sharma, S. S. Kanwar, A. Kumar, *Front. Plant Sci.* **2016**, *7*, 1667.
[17] H.-C. Ahn, S. Y. Lee, J. W. Kim, W. S. Son, C. G. Shin, B. J. Lee, *Mol. Cells* **2001**, *12*(1), 127.
[18] W.-H. Huang, A. R. Lee, P. Y. Chien, T. C. Chou, *J. Pharm. Pharmacol.* **2005**, *57*(2), 219.
[19] J.-M. Hwang, T. H. Tseng, Y. Y. Tsai, H. J. Lee, F. P. Chou, C. J. Wang, C. Y. Chu, *J. Biomed. Sci.* **2005**, *12*(2), 389.
[20] I. N. Kang, N. N. Nik Salleh, W. J. Chung, C. Y. Lee, S. C. Tan, *Processes* **2019**, *7*(12), 963.
[21] H. Takahashi, M. C. Chen, H. Pham, E. Angst, J. C. King, J. Park, E. Y. Brovman, H. Ishiguro, D. M. Harris, H. A. Reber, O. J. Hines, A. S. Gukovskaya, V. L. W. Go, G. Eibl, *Biochimica et Biophysica Acta (BBA)-Mol. Cell Res.* **2011**, *1813*(8), 1465.
[22] M. Gharbavi, B. Johari, N. Mousazadeh, B. Rahimi, M. P. Leilan, S. S. Eslami, A. Sharafi, *Mol. Biol. Rep.* **2020**, *47*(9), 6517.
[23] M. Gharbavi, B. Johari, S. S. Eslami, N. Mousazadeh, A. Sharafi, *Cell Biol. Int.* **2020**, *44*(12), 2485.
[24] M. Gharbavi, H. Danafar, A. Sharafi, *J. Biomed. Mater. Res. A* **2020**, *108*(8), 1688.
[25] Z. Chen, Q. Zhang, Q. Huang, Z. Liu, L. Zeng, L. Zhang, X. Chen, H. Song, J. Zhang, *Int. J. Pharm.* **2022**, *617*, 121578.
[26] M. Gharbavi, B. Johari, E. Rismani, N. Mousazadeh, A. H. Taromchi, A. Sharafi, *ACS Chem. Nerosci.* **2020**, *11*(24), 4499.
[27] H. A. Alhazmi, *Sci. Pharm.* **2019**, *87*(1), 5.
[28] L. Chan, L. He, B. Zhou, S. Guan, M. Bo, Y. Yang, Y. Liu, X. Liu, Y. Zhang, Q. Xie, T. Chen, *Chemistry–An Asian J.* **2017**, *12*(23), 3053.
[29] X. He, L. Pei, H. H. Y. Tong, Y. Zheng, *AAPS PharmSciTech* **2011**, *12*(1), 104.
[30] K. Hauner, P. Maisch, M. Retz, *Der Urologe. Ausg. A* **2017**, *56*(4), 472.
[31] G. Mohan, A. H. T P, J. A J, S. D. K M, A. Narayanasamy, B. Vellingiri, *J. Basic Appl. Zoology* **2019**, *80*(1), 1, 14.
[32] R. Wahab, M. A. Siddiqui, Q. Saquib, S. Dwivedi, J. Ahmad, J. Musarrat, A. A. al-Khedhairy, H. S. Shin, *Colloids Surf. B. Biointerfaces* **2014**, *117*, 267.
[33] D. Selvakumari, R. Deepa, V. Mahalakshmi, P. Subhashini, N. Lakshminarayan, *ARPN J. Eng. Appl. Sci* **2015**, *10*(12), 5418.
[34] Y. Wang, Y. Zhang, Y. Guo, J. Lu, V. P. Veeraraghavan, S. K. Mohan, C. Wang, X. Yu, *J. Photochem. Photobiol. B* **2019**, *201*, 111624.
[35] J. Iqbal, B. A. Abbasi, A. Munir, S. Uddin, S. Kanwal, T. Mahmood, *Microsc. Res. Tech.* **2020**, *83*(6), 706.
[36] U. Kanchana, T. V. Mathew, *Surf Interfaces* **2021**, *24*, 101056.
[37] N. Montero, E. Pérez, M. Benito, C. Teijón, J. M. Teijón, R. Olmo, M. D. Blanco, *Int. J. Pharm.* **2019**, *554*, 337.
[38] S. S. Elshama, M. E. Abdallah, R. I. Abdel-Karim, *Open Nanomed. J.* **2018**, *7*(1), 16.
[39] J. Iqbal, B. A. Abbasi, T. Yaseen, S. A. Zahra, A. Shahbaz, S. A. Shah, S. Uddin, X. Ma, B. Raouf, S. Kanwal, W. Amin, *Sci. Rep.* **2021**, *11*(1), 1.
[40] J. Schnitzer, P. Oh, *Am. J. Phys. Heart Circ. Physiol.* **1992**, *263*(6), H1872.
[41] C. Chaudhury, S. Mehnaz, J. M. Robinson, W. L. Hayton, D. K. Pearl, D. C. Roopenian, C. L. Anderson, *J. Exp. Med.* **2003**, *197*(3), 315.
[42] H. Birn, J. C. Fyfe, C. Jacobsen, F. Mounier, P. J. Verroust, H. Ørskov, T. E. Willnow, S. K. Moestrup, E. I. Christensen, *J. Clin. Invest.* **2000**, *105*(10), 1353.
[43] S. Cui, P. J. Verroust, S. K. Moestrup, E. I. Christensen, *Am. J. Physiol-Renal Physiol.* **1996**, *271*(4), F900.
[44] J. Schnitzer, A. Sung, R. Horvat, J. Bravo, *J. Biol. Chem.* **1992**, *267*(34), 24544.
[45] H. Sage, C. Johnson, P. Bornstein, *J. Biol. Chem.* **1984**, *259*(6), 3993.
[46] I. Cacciatore, E. Fornasari, L. Marinelli, P. Eusepi, M. Ciulla, O. Ozdemir, A. Tatar, H. Turkez, A. di Stefano, *Eur. J. Pharm. Sci.* **2017**, *109*, 402.
[47] M. Ahmari, A. Sharafi, J. Mahmoudi, I. Jafari-Anarkoli, M. Gharbavi, M. J. Hosseini, *J. Mol. Neurosci.* **2020**, *70*(10), 1639.
[48] M. Gharbavi, A. Sharafi, P. Motamed Fath, S. Oruji, H. Pakzad, H. Kheiri Manjili, *J. Appl. Biotechnol. Reports* **2021**, *8*(1).
[49] H. A. Ammar, M. S. Alghazaly, Y. Assem, A. Abou Zeid, *Env. Nanotechnol. Monitoring Manag.* **2021**, *16*, 100543.
[50] X. Fang, X. Wu, C.'. Li, B. Zhou, X. Chen, T. Chen, F. Yang, *RSC Adv.* **2017**, *7*(14), 8178.
[51] M. S. L. Pereira, F. Klamt, C. C. Thomé, P. V. Worm, D. L. de Oliveira, *Oncotarget* **2017**, *8*(13), 22279.
[52] D. Wu, Q. Liang, Z. Chen, *Luminescence* **2016**, *31*(4), 965.
[53] D. Usoltsev, V. Sitnikova, A. Kajava, M. Uspenskaya, *Biomolecules* **2020**, *10*(4), 606.
[54] S. N. Nyamu, L. Ombaka, E. Masika, M. Ng'ang'a, *J. Interdiscip. Nanomed.* **2019**, *4*(3), 86.
[55] A. R. Gardouh, S. Gad, H. M. Ghonaim, M. M. Ghorab, *J. Pharm. Res. Int.* **2013**, 326.
[56] R. Rajera, K. Nagpal, S. K. Singh, D. N. Mishra, *Biol. Pharm. Bull.* **2011**, *34*(7), 945.
[57] A. Y. Waddad, S. Abbad, F. Yu, W. L. L. Munyendo, J. Wang, H. Lv, J. Zhou, *Int. J. Pharm.* **2013**, *456*(2), 446.
[58] K. M. Tjørve, E. Tjørve, *PLoS ONE* **2017**, *12*(6), e0178691.
[59] G. Bisht, S. Rayamajhi, *Nanobiomedicine* **2016**, *3*(Godište 2016), 3.
[60] W. Yu, Y. Wang, J. Zhu, L. Jin, B. Liu, K. Xia, J. Wang, J. Gao, C. Liang, H. Tao, *Biomaterials* **2019**, *192*, 128.

[61] Y. Gong, X. Li, G. Liao, Y. Ding, J. Li, Y. Cao, *RSC Adv.* **2018**, *8*(28), 15380.
[62] G. Jiang, L. Zhang, J. Wang, H. Zhou, *Animal Cells Syst.* **2016**, *20*(5), 296.
[63] B. Liu, L. Ding, L. Zhang, S. Wang, Y. Wang, B. Wang, L. Li, *Am. J. Chin. Med.* **2019**, *47*(06), 1405.
[64] Z. YongHai, L. JunZhao, Z. XianFeng, G. GuangZhong, L. Jun, Z. Qin, D. YaSuo, *Int. J. Pharm.* **2019**, *15*(7), 844.
[65] S. Ostrovsky, G. Kazimirsky, A. Gedanken, C. Brodie, *Nano Res.* **2009**, *2*(11), 882.
[66] J. Jiang, J. Pi, J. Cai, *Bioinorg. Chem. Appl.* **2018**, *2018*(1), 1062562.

SUPPORTING INFORMATION

Additional supporting information can be found online in the Supporting Information section at the end of this article.

How to cite this article: M. Gharbavi, B. Johari, R. Ghorbani, H. Madanchi, A. Sharafi, *Appl Organomet Chem* **2022**, e6926. https://doi.org/10.1002/aoc.6926